Theory of Off-Center Displacements in Solid Solutions of Ionic Crystals*

ROBERT J. QUIGLEY AND T. P. DAS
Department of Physics, University of California, Riverside, California
(Received 23 January 1967; revised manuscript received 14 August 1967)

The minimum-energy configurations for impurity displacements along the ⟨111⟩, ⟨110⟩, and ⟨100⟩ crystal symmetry axes were determined for KCl:Li^+, KBr:Li^+, and CsF:Na^+, through calculations based on a nearest-neighbor Born-Mayer–type model. The off-center configurations were all found to have lower energies than the centrosymmetric configurations. For all three materials the ⟨111⟩ displacement gave the lowest and the ⟨100⟩ the highest minimum energy, in agreement with the KCl:Li^+ experimental results. The CsF:Na^+ potential wells were about twice as deep as those in KCl:Li^+, whereas the KBr:Li^+ wells were only half as deep, indicating rapid tunneling between adjacent minima, which might explain the absence of an electrocaloric effect in KBr:Li^+. The calculated static dipole moments of the ⟨111⟩ configurations were 6.23, 5.90, and 6.72 D, respectively, for KCl:Li^+, KBr:Li^+, and CsF:Na^+. The electric-field-gradient tensor was calculated at the impurity nucleus position for the three configurations. For the ⟨111⟩ configuration, the quadrupole coupling constants e^2qQ for Li^7 in KCl and KBr were -0.1196 Mc/sec and -0.0834 Mc/sec, respectively, and for Na^{23} in CsF it was 3.965 Mc/sec. An analysis of the expected quadrupole splittings of nuclear magnetic resonance (NMR) lines for various relative orientations of applied electric and magnetic fields indicates that such studies can distinguish between different possible minimum-energy configurations for these materials.

I. INTRODUCTION

SOLID solutions of ionic crystals have recently attracted considerable theoretical attention. Efforts have been made to explain macroscopic properties,[1] such as the heat of solution, or the ionic conductivity. The interpretation of other phenomena such as nuclear resonance[2] in solid solutions and electron resonance of paramagnetic ions,[3] dissolved in ionic crystals to reduce broadening effects, requires a definitive knowledge of the ionic configuration about the impurity.[4,5] Recently, by the use of several different experimental techniques, evidence[6–9] has accumulated that a novel type of lattice distortion occurs when the mismatch in size between the substituent and replaced ions is large. Thus when the small Li^+ ion is substituted for the K^+ ion in KCl, experiment suggests that the Li^+ ion shuttles around a number of equivalent off-site positions[6,10,11] leading to observable dielectric,[7,9] thermal,[9] and mechanical[8] effects. In this respect, the behavior of the Li^+ ion is similar to that of OH^- and CN^- ions dissolved in ionic crystals,[12] except that the entire dipole moment which accompanies the introduction of the Li^+ ion stems from the resulting lattice distortion and polarization, whereas the other two solute ions have intrinsic dipole moments. A first-principle analysis of the origin of off-center minima is of interest not only for the interpretation of the experimentally observed effects but also to test the adequacy of a model of the Born-Mayer type for this special situation and to obtain a basis for improvement of the theory.

The two systems which have received the most attention are KCl:Li^+ and KBr:Li^+. The electrocaloric experiments of Lombardo and Pohl[6] indicate that a dipole moment which can be aligned by an electric field accompanies the introduction of a Li^+ ion into KCl. The magnitude of this dipole moment can be estimated from the degree of electrocooling. No electrocaloric effect has been found for Li^+ in KBr. The dielectric dispersion measurements of Moriarity and Sack[7] provide additional support for the interpretation that Li^+ is off center in KCl:Li^+. The ultrasonic propagation and attenuation experiments of Byer and Sack[8] argue strongly in favor of impurity displacement

* Work supported by the National Science Foundation.

[1] B. G. Dick and T. P. Das, Phys. Rev. **127**, 1053 (1962); M. P. Tosi and M. Doyoma, *ibid.* **151**, 642 (1966).

[2] H. Kawamura, E. Otsuka, and K. Ishiwatari, J. Phys. Soc. Japan **11**, 1064 (1956); R. E. Slusher and E. L. Hahn, Phys. Rev. Letters **12**, 246 (1964); L. O. Andersson and E. Forslind, J. Chem. Phys. **38**, 2303 (1963); Arkiv Fysik **28**, 49 (1964); W. D. Ohlsen and M. Melich, Phys. Rev. **144**, 240 (1966).

[3] G. D. Watkins, Phys. Rev. **113**, 79 (1959); E. Feher, *ibid.* **136**, A145 (1964).

[4] B. G. Dick, Phys. Rev. **145**, 609 (1966); Y. Fukai, J. Phys. Soc. Japan **18**, 1413 (1963).

[5] T. P. Das, Phys. Rev. **140**, A1957 (1965); R. R. Sharma, thesis, University of California, Riverside, California (unpublished); G. D. Watkins, Phys. Rev. **113**, 79 (1959).

[6] G. Lombardo and R. O. Pohl, Phys. Rev. Letters **15**, 291 (1965), and Bull. Am. Phys. Soc. **11**, 213 (1966).

[7] H. S. Sack and M. C. Moriarity, Solid State Commun. **3**, 93 (1965).

[8] N. E. Byer and H. S. Sack, Phys. Rev. Letters **17**, 72 (1966); N. E. Byer, F. S. Welsh, and H. S. Sack, Bull. Am. Phys. Soc. **11**, 229 (1966).

[9] H. Bogardus and H. S. Sack, Bull. Am. Phys. Soc. **11**, 229 (1966). Thermal conductivity experiments have been carried out for both KCl:Li^+ and KBr:Li^+ by F. C. Bauman, J. P. Harrison, R. O. Pohl, and W. D. Seward, Phys. Rev. (to be published).

[10] S. P. Bowen, M. Gomez, J. A. Krumhansl, and J. A. D. Matthew, Phys. Rev. Letters **16**, 1105 (1966); M. Gomez, S. P. Bowen, and J. A. Krumhansl, *ibid.* **153**, 1009 (1967).

[11] M. E. Baur and W. R. Salzman, Phys. Rev. **151**, 710 (1966).

[12] A representative sample of the literature on the OH^- and CN^- materials is: U. Kuhn and F. Lüty, Solid State Commun. **2**, 281 (1964); **3**, 31 (1965); W. Känzig, H. R. Hart, and S. Roberts, Phys. Rev. Letters **13**, 543 (1964); I. Shepherd and G. Feher, *ibid.* **15**, 194 (1965); W. D. Seward and V. Narayanamurti, Phys. Rev. **148**, 463 (1966); G. Feher, I. W. Shepherd, and H. B. Shore, Phys. Rev. Letters **16**, 500 (1966); C. K. Chau, M. V. Klein, and B. Wedding, *ibid.* **17**, 521 (1966).

along a ⟨111⟩ axis. Sack and collaborators have carried out dielectric dispersion and absorption measurements[9] in the KCl:Li^+ system which can be interpreted by assuming a tunneling motion between equivalent ⟨111⟩ minima at a frequency corresponding to about 1 cm^{-1}. This interpretation is based on the theory for the dynamics of the problem by Bowen, Gomez, Krumhansl, and Matthew (BGKM).[10] The optical absorption experiments of Nolt and Sievers[13] indicate the presence of broad absorption bands at 40 and 17.8 cm^{-1}, respectively in the KCl:Li^+ and the KBr:Li^+ systems. The KCl:Li^+ absorption has been interpreted[10] as representing the frequency of localized vibrations associated with the eight potential wells which are, respectively, along the eight ⟨111⟩ directions.

Several attempts[14–17] have been made to explain the origin of such off-center displacements and further to understand qualitatively and even semiquantitatively the observed experimental results. The earliest theoretical analysis was worked out by Matthew.[14] In his model the Li^+ ion was assumed to have a potential-energy curve expressible as a sixth-order polynomial in the impurity displacment along a ⟨100⟩ direction. The surrounding lattice was held rigid and provided a perfectly cubic (O_h) environment at the substitutional (central) lattice site. The calculations were repeated for three values of the nearest-neighbor distance from the central site. The energy of the impurity ion was calculated by including the Coulomb and repulsive interactions as well as the electronic polarization induced in the surrounding lattice by the movement of of the Li^+ ion. Matthew's conclusion was that for both KCl and KBr the Li^+ impurity ion could have off-center minima along the ⟨100⟩ directions. Dienes, Hatcher, Smoluchowski, and Wilson[15] (DHSW) carried out a more elaborate calculation in which some of Matthew's restrictions were removed. The nearest neighbors were still required to move radially with respect to the central site, but three distortion parameters were used in order to allow a C_{4v} environment to develop about the substitutional site. The next-nearest neighbors were also allowed to relax radially, but only one distortion parameter was employed. The electronic polarization of the ions was treated self-consistently. In minimizing the impurity energy as a function of the Li^+ ion displacement, which we call ζ, they found a catastrophic decrease of the energy with increasing ζ. There was no evidence of a minimum. They ascribed this catastrophe to the weakness of the Born-Mayer repulsive potential relative to the large polarization force which develops at small interionic separations. They then managed to avoid collapse by fortifying the Born-Mayer potential with an arbitrary but steep linear term. This fortification led to an off-center minimum in the impurity energy curve along a ⟨100⟩ direction.

The purpose of the work reported in this paper is threefold. First, in order to apply the Born-Mayer model, we wanted to study carefully the origin of the polarization catastrophe found by DHSW and then remove it, if possible, within the framework of the Born-Mayer model. A careful analysis of the causes of the castastrophe has enabled us to find prescriptions for its removal. Thus, while it is clear that the Born-Mayer potential is expected to be quantitatively erroneous at short interionic separations, an equally or perhaps more important source of error is the somewhat unrealistic treatment of polarization. The unrealistically large polarization force can be averted by replacing the constant anion polarizability with one varying with interionic separation. The Born-Mayer-Verwey repulsive potential, which is stronger and probably more realistic than the Born-Mayer for interionic separations much smaller than the nearest neighbor distance r_a in the perfect crystal, can also eliminate the catastrophe. This potential has been applied by several authors[18] to problems involving defects in ionic crystals.

A second aim of the present work was to determine whether the Born-Mayer model with these modifications could provide a qualitative explanation of the experimental data. The potential energy was calculated for impurity displacements ζ along three symmetry axes, the ⟨111⟩, ⟨110⟩, and ⟨100⟩ directions of the rocksalt structure, in order to study if the impurity energy for these geometries had features indicating that a ⟨111⟩ minimum was the stablest configuration and if so, whether there could be significant tunneling between ⟨111⟩ minima. In addition to KCl:Li^+ and KBr:Li^+, calculations were also performed on the isomorphic CsF:Na^+ system, the Na^{23} nucleus being a convenient one to explore nuclear quadrupole effects. We have examined the nuclear quadrupole interaction for the impurity ion displaced in all three directions to determine what additional information about off-center configurations can be obtained from nuclear-resonance studies.

Finally, a less immediate but more basic purpose of our work is to pave the way for a more quantitative treatment of the whole problem by a quantum mechanical analysis[19] of the interaction between the electrons of the impurity and those of its nearest neighbors. This is important because the major inaccuracies of the Born-Mayer type calculation arise from the choice of the repulsive potential between the impurity ion M

[13] I. G. Nolt and A. J. Sievers, Phys. Rev. Letters **16**, 1103 (1966).
[14] J. A. D. Matthew, Cornell University Materials Science Center Report No. 373, 1965 (unpublished); Solid State Commun. **3**, 363 (1965).
[15] G. J. Dienes, R. D. Hatcher, R. Smoluchowski, and W. Wilson, Phys. Rev. Letters **16**, 25 (1966).
[16] R. J. Quigley and T. P. Das, Bull. Am. Phys. Soc. **12**, 351 (1967); G. J. Dienes, R. D. Hatcher, R. Smoluchowski, and W. D. Wilson, *ibid.* **12**, 351 (1967).
[17] R. J. Quigley and T. P. Das, Solid State Commun. **5**, 487 (1967).
[18] E. J. W. Verwey, Rec. Trav. Chim. **65**, 521 (1946); A. Scholz, Phys. Status Solidi **7**, 973 (1964).
[19] Per-Olov Löwdin, Advan. Phys. **5**, 1 (1956).

and the nearest neighbor X at separations significantly different from that in the pure MX crystal. In addition, the treatment of polarization effects in terms of ionic polarizabilities is oversimplified for the distorted configurations that accompany the off-center displacement of the impurity ion. A quantum-mechanical treatment of the interaction between the electrons of the impurity ion and those of the nearest-neighbor ions would obviate the need for an assumed repulsive potential and would automatically yield the polarization energy between M and X ions. The modifications that we have made within the framework of the Born-Mayer model for both the polarization and repulsive effects at short distances will have their counterparts in a quantum-mechanical treatment in terms of the hybridization of the electronic orbitals and the two-center-exchange and Coulomb interactions. The interactions between the X ions and their other neighbors could still be handled using a Born-Mayer form of repulsive potential since the distant ions are displaced much less from the normal lattice sites and are not as severely polarized. A mixed calculation, quantum mechanical for the interaction of the impurity ion with its nearest neighbors but Born-Mayer for all other interactions, would be rather elaborate, so one needs to be assured of the expected quantitative success of such a calculation. We believe that the qualitative success of the Born-Mayer calculations reported in this paper in explaining the KCl:Li^+ and KBr:Li^+ experimental data provides the necessary assurance.

In Sec. II the model, the choice of repulsive and polarization constants, and the algebra for deriving the impurity energy expression will be described. In Sec. III we consider the results of minimization of the impurity energy with respect to the lattice distortion parameters and analyze their relationship to experimental results. In Sec. IV the nuclear quadrupole interaction of the impurity ion will be considered and the information which such interactions can provide about the lattice configuration will be discussed.

II. MODEL AND PROCEDURE

To determine the actual direction of impurity displacement, one needs the spatial variation of the impurity energy as a function of the impurity displacement ζ and accompanying lattice distortion. This distortion will be different for each inequivalent position of the Li^+ ion so that the energy for a given position must be found by minimization with respect to variation of the displacements of all other ions in the lattice. Obtaining the desired energy variation by a continuous mapping over impurity positions would thus be an expensive project if more than the immediate surroundings of the impurity were allowed to relax and even when only the nearest neighbors are given complete freedom for displacement the calculation would still be rather laborious. The potential-energy variation obtained this way would be useful in the analysis of the three dimensional motion of the impurity and its surroundings, but the quantitative accuracy would be debatable in view of the inherent weaknesses of a point ion model. We have therefore chosen the three most plausible displacement directions for examination, namely, the ⟨111⟩, ⟨110⟩, and ⟨100⟩ axes of a perfect fcc lattice having the rocksalt structure. An off-center position along these axes has C_{3v}, C_{2v}, and C_{4v} symmetry, respectively. In these three directions the energy is studied as a function of the impurity displacement ζ and the configurations giving minimum energy are examined. The configuration of lowest energy is taken to be the physically most likely one. The energy curve in the vicinity of this minimum would provide the potential for the vibrational spectrum observed by Nolt and Sievers.[13]

The geometries corresponding to the three directions of impurity ion displacement are illustrated in Figs. 1–3. All displacements are measured in units of the nearest-neighbor distance r_a in the perfect crystal. The displacements of the nearest neighbors are assumed to be radial with respect to the *displaced* position of the impurity ion. Ideally, a greater degree of freedom should be allowed, but this choice seemed the best compromise between the requirements of computational economy and physical realism. A similar choice of displacement direction has also been made in earlier calculations of lattice distortion around impurities.[1,4] In the present case, it is certainly more realistic than requiring displacements to be toward the substitutional site. Again in the interests of simplicity and economy, only the impurity ion and its nearest neighbors were allowed to relax. We believe that the nearest neighbors are by far

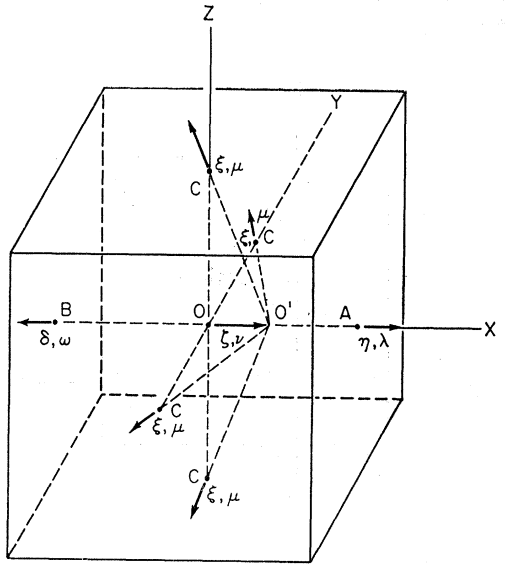

FIG. 1. Displacements ζ, ξ, η, and δ, and induced electronic dipoles ν, μ, λ, and ω for the ⟨100⟩ geometry. All displacements and induced dipoles are radial with respect to the displaced position of the impurity ion.

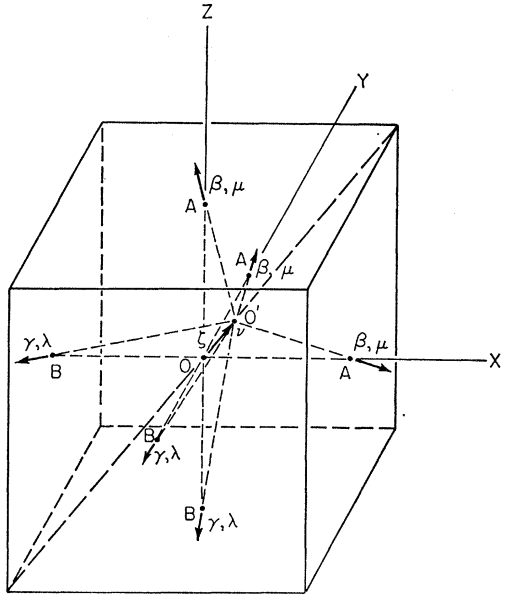

FIG. 2. Displacements ζ, β, and γ, and induced electronic dipoles ν, μ, and λ for the ⟨111⟩ geometry.

the most important agents producing off-center impurity displacement. Unfortunately, it is for the nearest-neighbor interactions that the Born-Mayer model is least applicable owing to the large displacements and polarizations which occur. We thus expect that the errors made in the evaluation of the nearest-neighbor contributions will overshadow the error resulting from neglect of contributions from the rest of the lattice. Consequently, the additional effort and computer time necessary for incorporation of more extensive lattice relaxation did not seem justifiable. Various second-nearest-neighbor effects were tested to determine if they might play a critical role. Thus in the ⟨100⟩ case, a calculation was tried which included repulsion between all pairs of the displaced ions (including next-nearest-neighbor repulsive forces) in order to determine if this could prevent the polarization catastrophe. The results showed that the catastrophe was not significantly affected. In the ⟨111⟩ case the influence of the (1,1,1) cation in KCl:Li^+ was estimated by allowing it to move and be polarized. Its influence was found to be negligible when a mesh size of 0.05 a_{KCl} was used and ζ was limited to 0.45 (a_{KCl} is the perfect crystal nearest-neighbor distance in KCl). It is conceivable that if the (1,1,1), (1,1,0) (1,0,1), and (0,1,1) ions all were allowed to relax and polarize, a significantly larger ⟨111⟩ impurity-ion displacement might result. But without a surer treatment of the interactions at large displacement, there is no assurance that such a larger value of ζ would be any more realistic. The next-nearest neighbors of the impurity will, however, play an important role in the calculation of electric field gradients at the positions of the nearest-neighbor nuclei.[4] In the present work, the field-gradient components at the position of the impurity ion are of most interest, so the neglect of next-nearest neighbors should be of little importance.

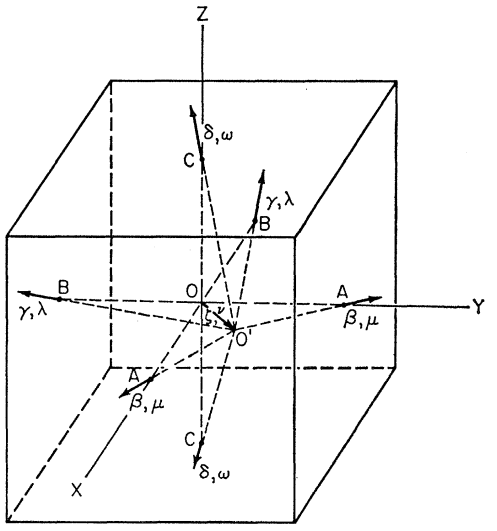

FIG. 3. Displacements ζ, β, γ, and δ, and induced electronic dipoles ν, μ, λ, and ω for the ⟨110⟩ geometry.

The repulsive potential between a pair of ions was taken to be of the Born-Mayer form, $R_{BM}(r) = A\exp(-r/\rho)$, where r is the interionic separation. Ideally, one would like to have a Li^+-Cl^- repulsive potential appropriate for the environment and interionic separations which exist in KCl:Li^+. However, such information does not currently exist and rather than make arbitrary adjustments we have simply chosen the repulsive constants derived from experimental work on LiCl. In view of this uncertainty, one cannot express a particular preference for any one of the various sets of repulsive constants available for LiCl and KCl. We have employed the repulsive parameters of Born and Huang,[20] since these have been used by several authors in the past. The values are listed in Table I. The Born-Mayer-Verwey potential was also used in the ⟨100⟩ KCl:Li^+ calculations to ascertain the influence of a repulsive potential which is stronger than the Born-Mayer potential at small interionic separations. The form of the Born-Mayer-Verwey potential is

$$\begin{aligned} R_{BMV}(r) &= A\exp(-r/\rho), \quad r \geq r_0 \\ &= B + C/r^{12}, \quad r \leq r_0. \end{aligned} \tag{1}$$

The repulsive constants A and ρ are the Born-Mayer values, while B and C are obtained from them by imposing continuity of the potential and its slope at r_0, the sum of the ionic radii. The repulsive energy was measured relative to that of a perfect KCl crystal. Only the repulsive potential between nearest neighbors was considered.

The polarizabilities were taken from the paper of

[20] M. Born and K. Huang, *Dynamical Theory of Crystal Lattices* (Oxford University Press, New York, 1954).

TABLE I. Constants used in the calculation of lattice distortion.

Crystal	Nearest-neighbor distance (Å)	Repulsive-force[a] parameter A (10^{-9} erg)	Repulsive-force[a] parameter ρ (Å)	Polarizability of positive ion[b] (Å^3)	Polarizability of negative ion[b] (Å^3)
KCl	3.147	3.63	0.324	1.33	2.96
LiCl	2.570	0.782	0.332	0.029	2.96
KBr	3.293	3.93	0.334	1.33	4.16
LiBr	2.751	0.821	0.348	0.029	4.16
CsF	3.005	8.09	0.284	3.34	0.64
NaF	2.317	1.11	0.288	0.41	0.64

[a] The repulsive parameters are taken from M. Born and K. Huang, *Dynamical Theory of Crystal Lattices* (Oxford University Press, London, 1954), p. 26.
[b] The polarizabilities were taken from J. R. Tessman, A. H. Kahn, and W. Shockley, [Phys. Rev. 92, 890 (1953)].

Tessman, Kahn, and Shockley[21] (TKS). The polarization catastrophe was found to be avoidable by use of a variable Cl^- polarizability, dependent upon the distance of the polarizing charge from the Cl^- ion. This choice of polarizability is reasonable because when a polarizing charge is inside a polarizable charge distribution it is much less effective than when it is outside. Quantum-mechanical calculations of the contributions to the polarizability from the various electronic states for both the Cl^- ion and the isoelectronic argon atom show[22] that nearly the entire polarizability of these systems comes from the $3s$ and $3p$ shells. In a semiclassical model, the $3s$ and $3p$ charge distributions can then be considered to constitute an outer shell in which all the polarizability of the ion resides. As the Li^+ ion penetrates this shell it will not be able to so completely polarize the shell as when it is outside. Thus a varying Cl^- polarizability was chosen, which is just the TKS polarizability for Li^+-Cl^- separations greater than the sum of the ionic radii and reduces to zero for very short interionic separations. For simplicity, a linear variation was taken for the intermediate region:

$$\begin{aligned} \alpha'(r)&=0, && r\leq r_1 \\ &=\left(\frac{r-r_1}{r_0-r_1}\right)\alpha_{Cl^-}, && r_1\leq r\leq r_0 \\ &=\alpha_{Cl^-}, && r\geq r_0 \end{aligned} \tag{2}$$

in which r_0 is the sum of the ionic radii and r_1 is the radius of the outermost maxima (nearly coincident) of the $3s$ and $3p$ anion valence electron wave functions.[23] In the actual calculations, the Cl^- ion was polarized by both the Li^+ ion and the rest of the lattice. Let $\mathbf{E}_1$ be the field due to the Li^+ ion and $\mathbf{E}_2$ that due to the rest of the lattice and suppose the Li^+ ion to be in the intermediate region ($r_1<r<r_0$). Then $\alpha_1=\alpha'(r)$ is the polarizability of the fraction A_1 of the anion inside the radius r, and $\alpha_2=\alpha_{Cl^-}-\alpha'(r)$ is the polarizability of the remainder of the anion, A_2. The dipole induced in A_2 is $\boldsymbol{\mu}_2=\alpha_2\mathbf{E}_2$ and that induced in A_1 is $\boldsymbol{\mu}_1=\alpha_1(\mathbf{E}_1+\mathbf{E}_2)$, so that the total dipole moment is $\boldsymbol{\mu}=\boldsymbol{\mu}_1+\boldsymbol{\mu}_2$. The corresponding self-energies are

$$U_1=\alpha_1\tfrac{1}{2}(\mathbf{E}_1+\mathbf{E}_2)^2=\alpha'(r)\tfrac{1}{2}(\mathbf{E}_1+\mathbf{E}_2)^2, \tag{3}$$

and

$$U_2=\tfrac{1}{2}\alpha_2\mathbf{E}_2^2=\tfrac{1}{2}[\alpha_{Cl^-}-\alpha'(r)]\mathbf{E}_2^2. \tag{4}$$

The total self-energy can then be written

$$U=U_1+U_2=[\mu_1^2/2\alpha'(r)]+\tfrac{1}{2}\mu_2^2[\alpha_{Cl^-}-\alpha'(r)]. \tag{5}$$

If the Li^+ ion is completely outside the Cl^- ion, then $\alpha'(r)=\alpha_{Cl^-}$, so $\alpha_2=0$, $\alpha_1=\alpha_{Cl^-}$, $\mu_2=0$, $\mu=\mu_1$, and $U=\mu^2/2\alpha_{Cl^-}$, as would be expected. By this partition of the polarizability, the polarizing fields due to both the Li^+ ion and the surrounding "nonpenetrating" lattice are then taken into account more realistically.

The dilute solid solution will be idealized as the limiting case of a lattice with a single impurity ion. In accordance with the conventions adopted in earlier literature on solid solutions, the energy will be measured relative to that of the perfect crystal and will be divided into three parts: the electrostatic energy ΔE_e arising from Coulomb interaction between all point charges; the polarization energy ΔE_p representing the sum of contributions from dipole-dipole interactions, dipole-monopole interactions and from the self-energies of the dipoles; and finally the repulsive energy ΔE_r from the nearest-neighbor repulsive interactions.

The ions of the lattice for the three cases displayed in Figs. 1–3 are grouped into two sets: D, the set of ions which are displaced, and L, the surrounding fixed ions of the lattice. The impurity ion will be designated by O'. The D ions were allowed to polarize but the surrounding L ions were assumed to be nonpolarizable. Since the impurity O' has the same charge as the ion it replaces, long-range polarization effects are expected to be small. Further, we use P to denote the set of dipoles associated with the ions of D, and primes will be used to indicate that the ion in question is displaced from the lattice site.

The electrostatic energy can be separated into three parts arising from three types of point-charge interactions: $D\leftrightarrow D$, $D\leftrightarrow L$, and $L\leftrightarrow L$, where no "self-interactions" are considered. The third type can be disregarded since it is independent of the displacements. The set of position vectors $\mathbf{r}_J$ of the lattice sites of the D ions will be denoted by R_D, and the set of displaced positions by R_D'. Then the change in electrostatic energy ΔE_e resulting from displacement of the D ions from lattice sites R_D to positions $R_{D'}$ is given by

$$\begin{aligned} \Delta E_e&=E(R_{D'})-E_e(R_D), \\ &=\sum_{J\in D}\sum_{K\in L} q_K q_J(1/r_{J'K}-1/r_{JK}) \\ &\quad+\sum_{\substack{J\in D\\ J\neq K}}\sum_{K\in D} q_J q_K(1/r_{J'K'}-1/r_{JK}), \end{aligned} \tag{6}$$

[21] J. R. Tessman, A. K. Kahn, and W. Shockley, Phys. Rev. 92, 890 (1953).
[22] M. Yoshimine and R. P. Hurst, Phys. Rev. 135, A612 (1964).
[23] D. R. Hartree and W. Hartree, Proc. Roy. Soc. (London) A156, 54 (1936).

in which q_J is the charge on ion J, $r_{JK}=|\mathbf{r}_J-\mathbf{r}_K|$, $\mathbf{r}_{J'K'}=|\mathbf{r}_{J'}-\mathbf{r}_{K'}|$, etc. All distances are measured in units of the nearest-neighbor distance r_a of the perfect lattice. Charges are measured in units of the proton charge $|e|$.

To convert the expression for ΔE_e into a more usable form, we superpose upon the distorted crystal virtual charge pairs $(\pm q_J)$. These pairs are placed at the lattice sites R_D left vacant by the lattice distortion. Half of these superposed charges will have the right sign to restore the perfect lattice, and this set of charges will be denoted by Q_D; the other half, denoted by the collective name $\bar{Q}_D$, will also be located at the R_D sites, but will have signs opposite to those of the corresponding D ions. Then, after some manipulation (shown in the Appendix), Eq. (6) can be split into a sum of interactions $D\leftrightarrow D$, $D\leftrightarrow\bar{Q}_D$, $\bar{Q}_D\leftrightarrow\bar{Q}_D$, and a second sum over interactions $q_J\leftrightarrow L_J$, where the sum is over the D ions and L_J represents a nearly perfect lattice whose one imperfection is the absence of ion J. Then

$$\Delta E_e=\sum_{\substack{J\in D\\ J\neq K}}\sum_{K\in D}q_Jq_K\left(\frac{1}{r_{J'K'}}+\frac{1}{r_{JK}}-\frac{1}{r_{J'K}}-\frac{1}{r_{JK'}}\right)+\sum_{J\in D}q_J\sum_{M\in L_J}\frac{q_M}{r_{J'M}}. \quad (7)$$

The last summation (over M) gives the potential in the vicinity of site $\mathbf{r}_J$ due to the surrounding perfect lattice L_J. This potential, which we will write as $V_L(\xi_J,\theta_J,\phi_J)$, is measured with respect to the Madelung potential at the lattice site $\mathbf{r}_J$ ($\xi_J=0$). It can be evaluated by various means such as those of Ewald,[24] Evjen,[24] or Nijboer and de Wette.[25] The Madelung potential itself is notoriously slow in its convergence, but the change in potential which occurs when the field point is moved off-center is much more rapidly convergent. One can take advantage of the symmetry of the cubic crystal and expand V_J (ξ_J,θ_J,ϕ_J) in the following manner:

$$V_L(\xi_J,\theta_J,\phi_J)=\sum_{l=1}^{\infty}r^l\varphi^{(l)}(\theta_J,\phi_J), \quad (8)$$

where

$$\varphi^{(l)}(\theta_J,\phi_J)=\sum_{m=-l}^{l}a_l{}^mY_l{}^m(\theta_J,\phi_J), \quad (9)$$

and

$$a_l{}^m=\frac{4\pi}{2l+1}\sum_i\frac{q_iY_l{}^{m*}(\theta_i,\phi_i)}{r_i{}^{l+1}}, \quad (10)$$

in which the sum on i is over the surrounding perfect lattice of charges q_i. We have excluded the $l=0$ term since it just gives the Madelung potential. Cubic symmetry restricts the summation over l to $l=4$, $l=6$, and higher even terms. The $l=4$ and $l=6$ terms give the potentials which have commonly been used in crystal field calculations for paramagnetic ions.[26] Since the coefficients $a_4{}^m$ depend on lattice sums falling off as r^{-5}, the convergence is expected to be much better than for the $1/r$ Madelung potential. This convergence is even better for higher l coefficients. The Evjen method, which for a sum over the first two Evjen cubes yields the Madelung constant to three significant figures, should give the $l=4$ and $l=6$ coefficients to at least four or five significant figures when a two-cube process is used. In our calculations the contributions of these lattice potentials V_L ordinarily constitute less than 10% of the total electrostatic energy. The $l=6$ term was found to be only 10% of the $l=4$ term and higher-order terms would be correspondingly less significant. We will therefore keep only the $l=4$ and $l=6$ terms in V_L. Since the potential V_L will be referred to frequently we write it down both in spherical polar and Cartesian coordinates:

$$\begin{aligned}V_L(\xi,\theta,\phi)&=7/16(-1.0275)\xi^4[35\cos^4\theta-30\cos^2\theta+3\\&\quad+5\cos4\phi\sin^4\theta]+3/64(-1.3339)\xi^6\\&\quad\times[231\cos^6\theta-315\cos^4\theta+105\cos^2\theta-5\\&\qquad-21\cos4\phi\sin^4\theta(11\cos^2\theta-1)], \quad (11)\end{aligned}$$

and

$$\begin{aligned}V_L(x,y,z)&=35/4(-1.0275)[x^4+y^4+z^4-\tfrac{3}{5}r^4]-21/2(-1.3339)\\&\quad\times\{x^6+y^6+z^6+15/4[x^4y^2+x^2y^4+x^4z^2\\&\qquad+x^2z^4+y^4z^2+y^2z^4]-(15/14)r^6\}. \quad (12)\end{aligned}$$

Expressions (11) and (12) apply in the vicinity of a vacant cation site, giving V_L due to the surrounding perfect crystal. For an anion site an over-all negative sign has to be introduced on the right-hand side of expressions (11) and (12). The numbers in parentheses would be just -1 if only the nearest neighbors were summed over in the evaluation of the coefficients. The final expression for the electrostatic energy is

$$\Delta E_e=\sum_{\substack{J\in D\\ J\neq K}}\sum_{K\in D}q_Jq_K\left(\frac{1}{r_{J'K'}}+\frac{1}{r_{JK}}-\frac{1}{r_{J'K}}-\frac{1}{r_{JK'}}\right)+\sum_{J\in D}q_JV_L(\xi_J,\theta_J,\phi_J). \quad (13)$$

The polarization energy can be broken down into four categories: $P\leftrightarrow P$, the dipole-dipole interaction; $P\leftrightarrow D$, the interaction of the dipoles with the displaced ions; $P\leftrightarrow L$, the interaction of the dipoles with the lattice ions L; and the self-energies of the dipoles. Using the same technique of superposition of virtual ion pairs $(Q_D+\bar{Q}_D)$ at the vacated sites R_D which was described

[24] P. P. Ewald, Ann. Physik **64**, 253 (1921); C. Kittel, *Introduction to Solid State Physics* (John Wiley & Sons, Inc., New York, 1966), 3rd ed., p. 95.

[25] B. R. A. Nijboer and F. W. de Wette, Physica **23**, 309 (1957).

[26] W. Low, *Paramagnetic Resonance in Solids* (Academic Press Inc., New York, 1960). See also R. S. Knox and A. Gold, *Symmetry in the Solid State* (W. A. Benjamin, Inc., New York, 1964).

earlier in conjunction with the electrostatic energy, one can restore the perfect lattice around a given vacant site $\mathbf{r}_J$ and find the interaction of the dipole with the lattice potential V_L (ξ_J,θ_J,ϕ_J). A compensating sum over $P\leftrightarrow\bar{Q}_D$ interactions must then be included, but is simple to carry out since it is over a finite number of dipoles and charges. Thus the ion-dipole interactions are reduced to the sum of three types of terms: $P\leftrightarrow D$, $P\leftrightarrow\bar{Q}_D$, and $\mathfrak{y}_J\leftrightarrow V_L(J)$, where J ranges over the D ions. On adding the dipole-dipole energy and dipole self-energy to the ion-dipole energy, the total polarization energy is given by

$$\Delta E_p=\sum_{\substack{K\in D\\K\neq J}}\sum_{J\in D} q_J\mathfrak{y}_K\cdot\nabla\left(\frac{1}{r_{K'J'}}-\frac{1}{r_{K'J}}\right)+\sum_{J\in D}\mathfrak{y}_J\cdot\nabla V_L(\xi_J,\theta_J,\phi_J)+\sum_{\substack{K\in D\\K\neq J}}\sum_{J\in D}\left[\frac{\mathfrak{y}_J\cdot\mathfrak{y}_K}{r_{J'K'}^3}-\frac{3(\mathfrak{y}_J\cdot\mathbf{r}_{J'K'})(\mathfrak{y}_K\cdot\mathbf{r}_{J'K'})}{r_{J'K'}^5}\right]+\sum_{J\in D}\frac{\mu_J^2}{2\alpha_J}. \quad (14)$$

The repulsive energy change is obtained by taking the difference between the pairwise sum of nearest neighbor repulsive energies in the distorted KCl:Li^+ lattice and the perfect KCl lattice. On carrying out this difference procedure one ends up with a summation over repulsive interactions associated with the set of ions D and their nearest neighbors N_J:

$$\Delta E_r=\sum_{J\in D}\sum_{K\in N_J}R(r_{J'K'})-\sum_{J\in D}\sum_{K\in N_J}R(r_{JK}). \quad (15)$$

In Eq. (15), $R(r_{JK})$ refers to the pairwise repulsive potential in the host lattice; $R(r_{JK})=A\exp(-r_{JK}/\rho)$ for the Born-Mayer approximation. In the first summation, one uses host lattice repulsive potentials in interactions not involving the impurity ion O', but for interactions involving O', the Born-Mayer parameters of the impurity-halide perfect crystal are used. A corresponding expression holds for the Born-Mayer-Verwey case.

The total impurity energy is then

$$\Delta E=\Delta E_e+\Delta E_p+\Delta E_r. \quad (16)$$

We next turn to the process of minimization of ΔE. The dipole moments in the energy expression ΔE appear only as linear and quadratic terms. By differentiating this expression with respect to each of the dipole moments and setting the results equal to zero, one can obtain a system of equations which are linear in the dipole moments and which are necessary conditions for an extremum in the energy relative to variation of the dipole moments. The solutions give the dipole moments as functions of the displacement parameters π_i (shown in Figs. 1–3). In order for these solutions to yield a minimum in the energy relative to variation of the moments, it is necessary for the determinant

$$|M_{ij}|=\left|\frac{\partial^2\Delta E}{\partial\mu_i\partial\mu_j}\right| \quad (17)$$

and its principal minors to be greater than zero. For all sets of displacement parameter values π_i investigated, this condition was met. The dipole moments were thus found in terms of the displacement parameters π_i and ΔE could then be expressed completely in terms of these parameters. This reduced the problem to one involving only four minimization parameters in the ⟨100⟩ and ⟨110⟩ calculations and three in the ⟨111⟩ case. This procedure is equivalent to a self-consistent evaluation of the dipole moments given by the equations[1]

$$\mu_i=\alpha_iE_i(\pi_1,\cdots,\pi_i,\cdots;\mu_1,\cdots,\mu_i,\cdots). \quad (18)$$

The equilibrium configuration was then determined by a direct minimization of $\Delta E(\pi_i)$. The numerical minimization procedure was essential, since a simple expansion in quadratic powers of the impurity displacement parameter ζ which would have led to linear equations on minimization, cannot yield off-center displacement. The minimization procedure itself was straightforward: the energy was evaluated for $(10)^p$ ionic configurations corresponding to likely values of the p displacement parameters, and the lowest energy for each value of the impurity displacement ζ was plotted. The number of parameters p was four in the ⟨100⟩ and ⟨110⟩ cases and three for the ⟨111⟩ calculations. The procedure was first carried out for mesh size increments of 0.05 r_a in the parameters. Subsequently, the mesh size was reduced to 0.01 r_a. Still further resolution could have been gained, but it was not felt that the results would be of any greater quantitative significance. In the KBr:Li^+ case a 0.05 r_a mesh gave the same minimum energy, −0.673 eV, for all three directions and a mesh size of 0.01 r_a was necessary in order to distinguish between the energy minima for the three directions.

III. RESULTS ON EQUILIBRIUM CONFIGURATIONS AND DIPOLE MOMENTS

The results for the three impurity-displacement directions are given in Table II for the KCl:Li^+, KBr:Li^+, and CsF:Na^+ systems and are plotted in Figs. 5-7. In all three systems the ⟨111⟩ axis has the deepest minimum, the ⟨100⟩ axis the most shallow, and the ⟨110⟩ a minimum which is intermediate. One can attempt to justify this order of the minima in the three directions as follows. The components of electric fields due to "A" ions (see Figs. 1–3) in the displacement direction are in the ratio of $1:1/\sqrt{2}:1/\sqrt{3}$ for ⟨100⟩, ⟨110⟩, and ⟨111⟩, respectively, for small displacements. However, the number of A ions in the three cases are in the ratio of 1:2:3. Taking the products of these two factors, one obtains the ratio $1:\sqrt{2}:\sqrt{3}$. While there

TABLE II. Displacements and dipole moments of minimum energy configurations.

Material	Direction	Ion type	Number	Displacement (r_a)	Dipole moment ($\|e\|r_a$)	Total energy (eV)	Total dipole moment (debye)
KCl:Li^+	⟨111⟩	(0,0,0)	1	0.19	0.0005	−0.780	6.23
		(1,0,0)	3	−0.09	0.0216		
		(1̄,0,0)	3	0.01	−0.0284		
	⟨110⟩	(0,0,0)	1	0.16	−0.0005	−0.772	5.53
		(1,0,0)	2	−0.10	0.0266		
		(0,0,1)	2	−0.04	−0.0132		
		(1̄,0,0)	2	0.01	−0.0285		
	⟨100⟩	(0,0,0)	1	0.12	0.0005	−0.762	4.14
		(1,0,0)	1	−0.10	−0.0322		
		(1̄,0,0)	1	0.01	−0.0295		
		(0,1,0)	4	−0.05	−0.0120		
KBr:Li^+	⟨111⟩	(0,0,0)	1	0.17	0.0004	−0.684	5.90
		(1,0,0)	3	−0.08	0.0221		
		(1̄,0,0)	3	0.00	−0.0329		
	⟨110⟩	(0,0,0)	1	0.14	−0.0002	−0.680	4.81
		(1,0,0)	2	−0.09	0.0132		
		(0,0,1)	2	−0.04	−0.0129		
		(1̄,0,0)	2	0.00	−0.0281		
	⟨100⟩	(0,0,0)	1	0.10	0.0003	−0.675	3.56
		(1,0,0)	1	−0.08	0.0268		
		(1̄,0,0)	1	0.00	−0.0328		
		(0,1,0)	4	−0.05	−0.0126		
CsF:Na^+	⟨111⟩	(0,0,0)	1	0.21	0.0094	−0.952	6.72
		(1,0,0)	3	−0.13	0.0070		
		(1̄,0,0)	3	0.03	−0.0081		
	⟨110⟩	(0,0,0)	1	0.18	−0.0138	−0.936	5.58
		(1,0,0)	2	−0.14	0.0084		
		(0,0,1)	2	−0.03	−0.0040		
		(1̄,0,0)	2	0.03	−0.0073		
	⟨100⟩	(0,0,0)	1	0.12	0.0102	−0.886	4.37
		(1,0,0)	1	−0.15	0.0118		
		(1̄,0,0)	1	0.02	−0.0076		
		(0,1,0)	4	−0.04	−0.0036		

is no direct experimental evidence to check the relative depths of the ⟨100⟩ and ⟨110⟩ minima, the fact that they both come out more shallow than ⟨111⟩ is in qualitative agreement with the ultrasonic measurements of Byer and Sack.[8]

In the ⟨100⟩ KCl:Li^+ calculations using the Born-Mayer potential and a constant polarizability, the minimum was found to be shallow with a depth of 0.013 eV relative to the on-site energy and was found at a reasonable distance, $\zeta=0.12$, off-center, but for larger values of ζ a catastrophic decrease of the energy occurred which resembled that found by DHSW in their original calculations for KCl:Li^+ ⟨100⟩. As explained in an earlier paper,[17] the catastrophe was found to be avoidable by use of the varying anion polarizability described in Sec. II. The results of the ⟨100⟩ KCl:Li^+ calculations are plotted in Fig. 4(a). It is seen that use of either the variable anion polarizability or of the Born-Mayer-Verwey potential will eliminate the catastrophe, but that adoption of the Born-Mayer-Verwey potential results in a steeper energy curve than use of the varying polarizability does. An important point is that all of the curves which incorporate polarization have nearly identical minima which demonstrates that the minimum is insensitive to the measures employed to remove the catastrophe. To demonstrate the general nature of the polarization catastrophe, the lattice energy in pure KCl was calculated as a function of the ⟨100⟩ displacement of a single K^+ ion. In Fig. 4(b) the ⟨100⟩ KCl:K^+ results are plotted for the case of Born-Mayer repulsion with TKS polarizabilities (curve A′) and with zero polarizabilities (curve B′). The KCl lattice is thus seen to be metastable according to the unmodified (constant polarizabilities) Born-Mayer model, although the minimum predicted is at the lattice site.

We encountered no catastrophe in either the ⟨111⟩ or ⟨110⟩ calculations for KCl:Li^+, KBr:Li^+, and CsF:Na^+, out to impurity ion displacements of $\zeta\leq 0.45$ r_a. One could suspect that the absence of catastrophe may partly be attributed to the exclusion of the (1,1,1) ion from consideration in the ⟨111⟩ calculations and correspondingly the (1,1,0) ion in the ⟨110⟩ calculations. In the ⟨111⟩ KCl:Li^+ case, an estimate of the influence of the approached (1,1,1) ion was made by allowing it to relax and polarize as freely as the D ions, and again no abrupt polarization increase occurred for $\zeta\leq 0.45$ r_a. These results can be rationalized by examination of the

geometries of the three displacement direction configurations, shown in Figs. 1–3. Thus in the ⟨111⟩ case, the three A ions can effectively shield the (1,1,1) ion from the approaching impurity, thus safeguarding against a polarization catastrophe; a similar argument applied to the two A ions in ⟨110⟩ geometry. Since for small displacements, the O'C directions are effectively perpendicular to the ⟨100⟩ displacement directions $O'A$, the C ions cannot substantially shield the (1,0,0) ion from the impurity and are ineffective in preventing polarization catastrophe.

Since the ⟨111⟩ and the ⟨110⟩ minima are deeper than the ⟨100⟩, it appears reasonable that some sort of tunneling mode[10] may enable the impurity ion to shuttle back and forth from say the [111] minimum to the [11$\bar{1}$] minimum by a route which is contained in the $x=y$ plane, and which passes through the [110] minimum. The KBr:Li$^+$ minima for all three directions were shallower than those of the KCl:Li$^+$ system. In the calculations carried out over a 0.05 r_a mesh, the energies of the three minima were nearly identical, the differences being less than 0.001 eV. For the 0.01 r_a mesh calculations, the energy differences were uniformly

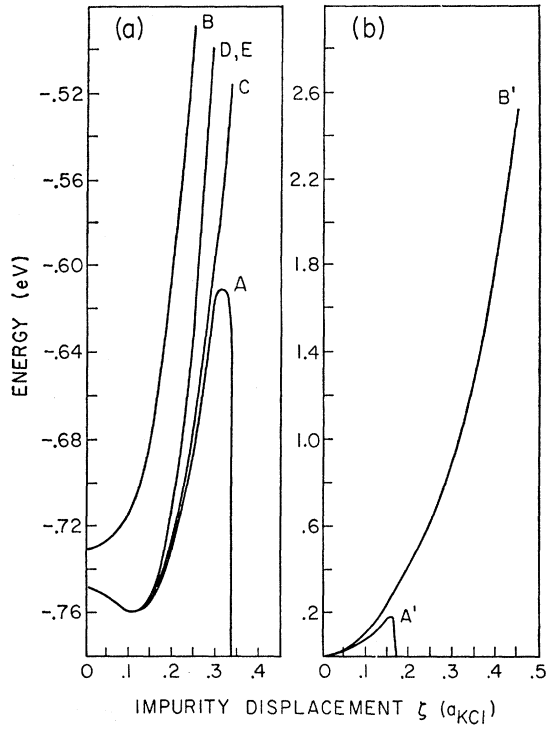

FIG. 4. Lattice energies as a function of the displacement of the impurity ion. (a) KCl:Li$^+$ energies for the ⟨100⟩ cases: A—Born-Mayer repulsion and fixed Cl$^-$ polarizability; B—Born-Mayer repulsion but no electronic polarization; C—Born-Mayer repulsion and varying Cl$^-$ polarizability; D—Born-Mayer-Verwey repulsion and fixed Cl$^-$ polarizability; E—Born-Mayer-Verwey repulsion and varying anion polarizability. (b) KCl:K$^+$ energies for two corresponding ⟨100⟩ cases: A′—Born-Mayer repulsion and fixed Cl$^-$ polarizability; B′—Born-Mayer repulsion and no electronic polarization. The polarization catastrophe occurs in A and A′.

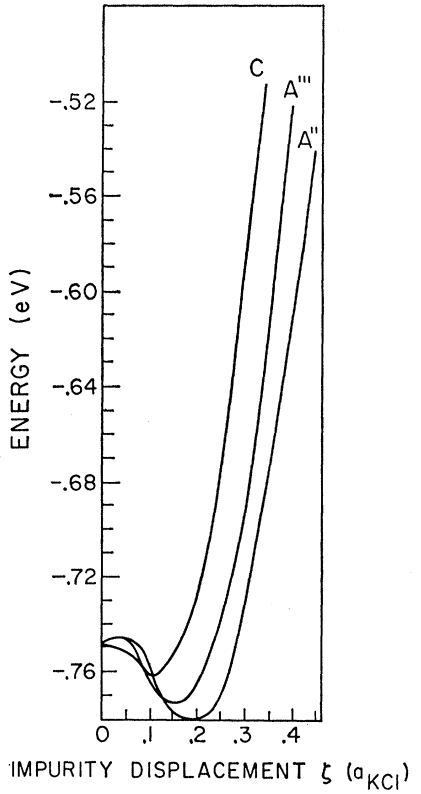

FIG. 5. Comparison of the KCl:Li$^+$ lattice energy curves for impurity displacements along three symmetry directions: A″—⟨111⟩ case; A‴—⟨110⟩ case; C—⟨100⟩ case [which is identical to curve C in Fig. 4(a)]. The ⟨111⟩ and ⟨110⟩ results plotted here are for Born-Mayer repulsion and fixed Cl$^-$ polarizability. No polarization catastrophe occurs.

very nearly one-half the corresponding values in KCl:Li$^+$, as also were the depths measured relative to the energy of the centrosymmetric configuration. All barriers for angular motion in KBr:Li$^+$ therefore appear to be a factor of two lower than for KCl:Li$^+$. Thus the tunneling frequency between adjacent ⟨111⟩ directions for KBr:Li$^+$ is expected to be substantially larger than for KCl:Li$^+$. This, at least approximately follows the experimental trend, since no electrocaloric effect has been observed in the KBr:Li$^+$ system.[6]

The results for CsF:Na$^+$, on the other hand, suggest that tunneling will be less pronounced, since the barriers are about twice as high as those calculated for KCl:Li$^+$, and the mass of the Na$^+$ ion is about three times that of the Li$^+$ ion. One might therefore expect the electrocaloric effect to be more pronounced and perhaps observable at higher temperatures than liquid helium.

The calculated dipole moments for the entire distorted lattice are given in Table II, for each material and each geometry. In KCl:Li$^+$, the dipole moment along the ⟨111⟩ direction for ζ along ⟨111⟩, is 6.23 D. This is only in order of magnitude agreement with Lombardo and Pohl's value of 2.54 D which was

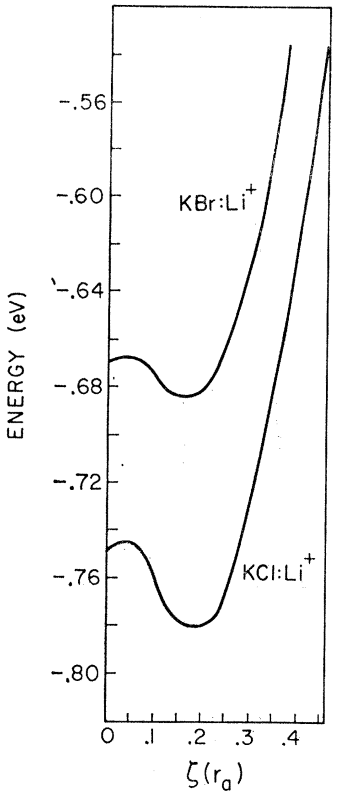

FIG. 6. Comparison of the ⟨111⟩ results for the KCl:Li^+ and KBr:Li^+ systems, illustrating the greater depth of the KCl:Li^+ minimum. In Fig. 7 the still deeper Na^+:CsF ⟨111⟩ energy curve is plotted. The impurity displacement ζ is measured in units of r_a, the perfect crystal nearest neighbor distance.

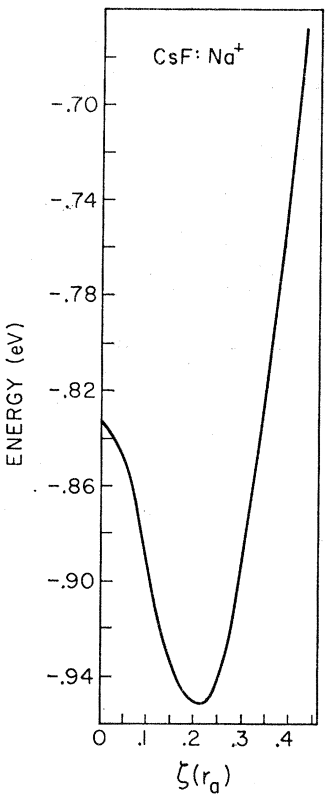

FIG. 7. Lattice energy curve as a function of impurity displacements ζ for CsF:Na^+, with ζ along the ⟨111⟩ direction. The energy scale is the same as that of Fig. 6.

derived using a Lorentz local field. Our dipole moment value comes mainly from the ionic displacements of the Li^+ ion and its nearest neighbors, the contribution from the electronic dipoles being in some cases an order of magnitude smaller.

One can make a rough estimate of localized mode frequencies by fitting our calculated energy curves to parabolic (harmonic oscillator) potentials. For KCl:Li^+ we find that for oscillation along the ⟨111⟩ direction, the potential can be fitted quite well in the form $V(x) = \frac{1}{2}kx^2$ where $k = m\omega^2$ and x is the displacement from the minimum. Using for the mass of the oscillating particle the lithium mass, we get $\nu/c = (1/2\pi c)(k/m)^{\frac{1}{2}} = 154$ cm^{-1}. The analogous frequenciy for KBr:Li^+ is 119 cm^{-1}. These values are considerably higher than the experimentally observed absorption frequencies[13] of 40 and 17.8 cm^{-1}. An even rougher estimate can be made of the frequency of vibration transverse to the ⟨111⟩ direction. The presumed potential well extends from the ⟨111⟩ minimum to the adjacent ⟨110⟩ minimum; we assume it to be a harmonic oscillator potential centered at the ⟨111⟩ minimum and determine its curvature by a fit to the ⟨110⟩ energy. This gives for the KCl:Li^+ system a vibrational frequency of 72 cm^{-1} and for KBr:Li^+, 51 cm^{-1}. These frequencies are closer to the experimental values and suggest that a precise treatment using a realistic potential may give values near those observed experimentally. For this one needs the local potential about the ⟨111⟩ minimum fairly accurately. Tunneling frequencies could then be found through the procedure of Bowen, Gomez, Krumhansl, and Matthew,[10] using three-dimensional harmonic-oscillator functions appropriate to the energy curves. We do not believe that our present energy curves are sufficiently quantitative to justify carrying out such a procedure, even though doing so might enable us to adjust the results to agree with experiment and thus work back to a better repulsive potential. As pointed out in the Introduction, the basic aim of our program is to obtain a first principle quantitative interpretation of the properties of these systems. We feel that quantitatively reliable results would require quantum mechanical calculations involving the explicit inclusion of covalency and overlap effects. Since the aim of our present semiclassical work was primarily to test the over-all features of the model, we have chosen not to parametrize the repulsive potentials to fit experimental results.

In summary, for our simple model the ⟨111⟩ axis falls out naturally as the displacement direction, the KBr:Li^+ potential barriers are found to be substantially less than those of KCl:Li^+, and the KCl:Li^+ dipole moment value is a little over twice the experimental value. These results lend credibility to the semiquantitative validity of the point-ion model.

IV. NUCLEAR QUADRUPOLE INTERACTION OF THE IMPURITY NUCLEUS

In this section we analyze nuclear quadrupole interaction effects due to the distortion of the lattice in the vicinity of the Li^+ ion. Both the impurity nucleus and neighboring ion nuclei should be subject to quadrupole effects arising out of the lattice distortion and polarization. The impurity nucleus is of critical importance since it would have no quadrupole interaction if it remained in a position of octahedral symmetry while the neighboring nuclei would still display quadrupole effects.[4] We therefore concentrate on the quadrupole interaction of the impurity nucleus.

The Hamiltonian for the interaction between the nuclear quadrupole moment and the potential field in the crystal can be written as[27]

$$H_Q = e^2\mathbf{Q}:\nabla\mathbf{E} = e^2\sum_{i,j} Q_{ij}(\nabla\mathbf{E})_{ij}, \tag{19}$$

where

$$(\nabla\mathbf{E})_{ij} = -\frac{\partial^2 V}{\partial x_i \partial x_j}, \tag{20}$$

and

$$Q_{ij} = \frac{eQ}{I(2I-1)}\left[\tfrac{3}{2}(I_jI_k+I_kI_j)-\delta_{jk}\mathbf{I}^2\right], \tag{21}$$

in which i, j stand for the Cartesian coordinate axes and the scalar quadrupole moment Q is related to the nuclear wave function:

$$Q = \int \Psi_{I,M_I=I}(4\pi/5)^{1/2}\sum_j r_j^2 Y_2^0(\theta_j,\varphi_j)\Psi_{I,M_I=-I}d\tau_N. \tag{22}$$

In a principal-axis system for the field-gradient tensor, the off-diagonal components are zero:

$$V_{x'y'} = V_{y'z'} = V_{z'x'} = 0. \tag{23}$$

The usual conventions for the labeling of the principal axes is that

$$|V_{x'x'}| \leq |V_{y'y'}| \leq |V_{z'z'}|. \tag{24}$$

Since Laplace's equation gives

$$V_{x'x'}+V_{y'y'}+V_{z'z'} = 0, \tag{25}$$

only two independent components remain which can be expressed in terms of the two quantities q and η:

$$q = V_{z'z'}, \quad \eta = (V_{x'x'}-V_{y'y'})/V_{z'z'}. \tag{26}$$

We next have to decide on the principal-axis systems for the geometries of interest and calculate the appropriate q and η.

The choice of principal axes is often dictated by symmetry. Cohen and Reif[27] have summarized the rules of selection of principal-axis orientation. From consideration of the reflection and rotational symmetries characterizing the geometries of Figs. 1–3, the unit vectors $\mathbf{e}_i$ for the principal axes with $i=1$, 2, 3 corresponding to x', y', and z' are given by

	$\mathbf{e}_1$	$\mathbf{e}_2$	$\mathbf{e}_3$
[111]	$1/\sqrt{2}(-1,0,1)$	$(\frac{2}{3})^{1/2}(\frac{1}{2},-1,\frac{1}{2})$	$1/\sqrt{3}(1,1,1)$,
[110]	$1/\sqrt{2}(1,1,0)$	$(0,0,1)$	$1/\sqrt{2}(1,-1,0)$,
[100)	$(0,1,0)$	$(0,0,1)$	$(1,0,0)$,

(27)

where the components in (27) are with respect to the coordinate system illustrated in Figs. 1–3. The direction cosines which are most useful in the calculation of principal components are given in Table III.

For the calculation of the field-gradient components at the displaced impurity sites, it is again convenient to use a superposition of equal and opposite charges $(Q_D+\bar{Q}_D)$ as was done in Sec. II. The surroundings of the impurity ion can then be split up into two parts: (1) a perfect lattice; and (2) a combination of displaced D ions, P dipoles, and charges $\bar{Q}_D$ (of opposite to normal sign) at the lattice sites. The field gradient V_{ij}^L due to the perfect lattice, is termed the lattice contribution and is obtained by differentiation of the appropriate lattice potential V_L, which was introduced in Sec. II. From the cubic symmetry of the perfect lattice, one expects zero field gradient at the substitutional site, but not at the displaced position of the impurity. The contribution from D, P, and $\bar{Q}_D$ is denoted by V_{ij}^N and is referred to as the distortion contribution. For purposes of a more detailed understanding of the origin of the field gradient, we decompose V_{ij}^N into two parts: V_{ij}^{NM} due to the neighboring monopoles, and V_{ij}^{ND} due to the dipoles.

On differentiating the expression for V_L in Eq. (12) at a point $\zeta=(x,y,z)$ away from the lattice site, one

TABLE III. Direction cosines between principal-axis systems and crystal cubic axes.

	[111]	[110]	[100]
$\alpha_{x'x}$	$-1/\sqrt{2}$	$1/\sqrt{2}$	0
$\alpha_{x'y}$	0	$1/\sqrt{2}$	1
$\alpha_{x'z}$	$1/\sqrt{2}$	0	0
$\alpha_{y'x}$	$\frac{1}{2}\sqrt{\frac{2}{3}}$	0	0
$\alpha_{y'y}$	$-\sqrt{\frac{2}{3}}$	0	0
$\alpha_{y'z}$	$\frac{1}{2}\sqrt{\frac{2}{3}}$	1	1
$\alpha_{z'x}$	$1/\sqrt{3}$	$1/\sqrt{2}$	1
$\alpha_{z'y}$	$1/\sqrt{3}$	$-1/\sqrt{2}$	0
$\alpha_{z'z}$	$1/\sqrt{3}$	0	0

[27] M. H. Cohen and F. Reif, in *Solid State Physics*, edited by F. Seitz and D. Turnbull (Academic Press Inc., New York, 1957), Vol. 5.

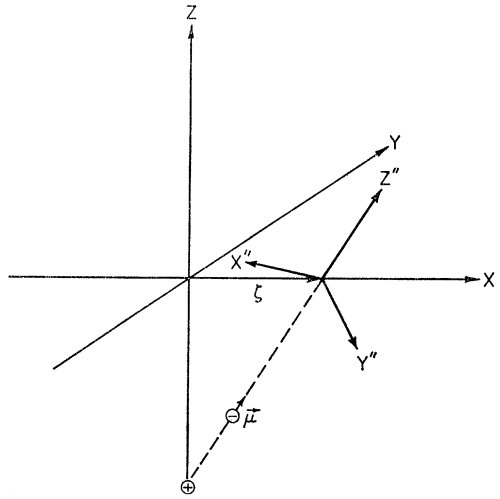

FIG. 8. Example of the principal axis (double-primed) system used in evaluating the electric field gradient at the displaced impurity position (shown here to be on the [100] axis), due to a displaced anion, its dipole $\mathfrak{y}$, and the virtual positive charge on the respective lattice site. The system is axial so that $V_{x''x''}=V_{y''y''}=-\frac{1}{2}V_{z''z''}$.

obtains

$$V_{ii}{}^{L}=\frac{\partial^2 V_L}{\partial x_i{}^2}=\frac{12}{5}A_L[3x_i{}^2-r^2]+15B_L\Big[2x_i{}^4+3x_i{}^2(x_j{}^2+x_k{}^2)+\tfrac{1}{2}(x_j{}^4+x_k{}^4)-\frac{12}{7}x_i{}^2r^2-\frac{3}{7}r^4\Big], \quad (28)$$

$$V_{ij}{}^{L}=\frac{\partial^2 V_L}{\partial x_i\partial x_j}=\frac{-24}{5}A_L x_i x_j+30B_L\Big[x_i{}^3x_j+x_ix_j{}^3-\frac{6}{7}x_ix_jr^2\Big], \quad (29)$$

where (i,j,k) is a cyclic permutation of (1,2,3), $A_L=-8.9906$, and $B_L=14.006$. Equations (28) and (29) are with respect to the crystalline axis system, which we can then transform to the appropriate principal-axis system by using

$$V_{i'j'}=\sum_{i,j}\alpha_{i'i}\alpha_{j'j}V_{ij}, \quad (30)$$

where $\alpha_{i'i}$ denotes the direction cosines in Table III.

The distortion terms $V_{ij}{}^{N}$ involve summations over only a finite number of point charges and electronic dipoles. Our choice of radial displacements and electronic dipoles makes the calculation of the contributions to $V_{ij}{}^{N}$ from the displaced neighbor ions particularly simple. Thus, the neighboring ion J produces an axially symmetric tensor at the impurity O' with components

$$V_{z''z''}{}^{J}=q_J\Big(\frac{2}{r_{J'0'}{}^3}-\frac{2}{r_{J0'}{}^3}\Big)-\frac{6\mu_J}{r_{J'0'}{}^4}, \quad (31)$$
$$V_{x''x''}{}^{J}=V_{y''y''}{}^{J}=-\tfrac{1}{2}V_{z''z''}{}^{J},$$

the axis of symmetry Z'' being in the direction $O'J$. The geometry for a particular ion J is illustrated in Fig. 8 for the [100] case. One can then apply the simplified version of Eq. (30) for any axially symmetric tensor, namely,

$$V_{i'i'}=V_{z''z''}(\tfrac{3}{2}\alpha_{i'z''}{}^2-\tfrac{1}{2}), \quad (32)$$

to transform to the principal-axis system $i'=x', y', z'$. From each of the neighbors J, one could obtain off-diagonal components in this principal-axis system. However, on adding all the contributions, the off-diagonal components vanish and we have

$$V_{i'i'}=V_{i'i'}{}^{L}+V_{i'i'}{}^{NM}+V_{i'i'}{}^{ND}. \quad (33)$$

The results of our calculations for three displacement geometries (⟨111⟩, ⟨110⟩, and ⟨100⟩) and the three materials KCl:Li^+, KBr:Li^+, and CsF:Na^+ are given in Table IV.

In earlier work on nuclei adjacent to the impurity ion in solid solutions, $V_{i'i'}{}^{L}$ was ignored since it has a quadratic dependence on the displacement parameters

TABLE IV. Field-gradient components.[a]

	$V_{z'z'}{}^{L}$	$V_{x'x'}{}^{L}$	$V_{y'y'}{}^{L}$	$V_{z'z'}{}^{NM}$	$V_{x'x'}{}^{NM}$	$V_{y'y'}{}^{NM}$	$V_{z'z'}{}^{ND}$	$V_{x'x'}{}^{ND}$	$V_{y'y'}{}^{ND}$	$V_{z'z'}$	$V_{x'x'}$	$V_{y'y'}$
						KCl:Li^7						
[111]	0.965	−0.483	−0.483	1.654	−0.827	−0.827	0.263	−0.131	−0.131	2.882	−1.441	−1.441
[110]	−0.836	0.308	0.528	−0.794	0.111	0.682	−0.420	−0.047	0.467	−2.049	0.372	1.678
[100]	−0.631	0.315	0.315	−0.624	0.312	0.312	0.572	−0.286	−0.286	−0.682	0.341	0.341
						KBr:Li^7						
[111]	0.785	−0.393	−0.393	1.278	−0.639	−0.639	0.239	−0.120	−0.120	2.302	−1.151	−1.151
[110]	−0.639	0.230	0.409	−0.567	0.063	0.503	−0.361	−0.055	0.416	−1.567	0.239	1.328
[100]	−0.436	0.218	0.218	−0.251	0.126	0.126	−0.398	0.199	0.199	−1.086	0.543	0.543
						CsF:Na^{23}						
[111]	1.159	−0.579	−0.579	2.466	−1.233	−1.233	0.109	−0.055	−0.055	3.733	−1.867	−1.867
[110]	−1.060	0.401	0.660	−1.643	0.107	1.536	−0.175	−0.015	0.190	−2.878	0.493	2.386
[100]	−0.631	0.315	0.315	−1.648	0.824	0.824	−0.271	0.135	0.135	−2.549	1.275	1.275

[a] Units of e/a^3, where a is the nearest-neighbor separation.

which were quite small. In view of the sizable impurity displacement in the present work the values of $V_{i'i'}{}^{L}$ and $V_{i'i'}{}^{N}$ are comparable at the impurity nucleus as seen from Table IV. The dipolar contributions $V_{i'i'}{}^{ND}$ are found to be significantly smaller than the monopolar results $V_{i'i'}{}^{NM}$ but increase in importance in the order fluoride, chloride, and bromide neighbors, as one would expect from the increasing dipole polarizabilities.

In determining the quadrupole interaction energy of the impurity nucleus, one must take into account the Sternheimer antishielding effect.[28] The pertinent antishielding factors $(1-\gamma_\infty)$ for Li^+ and Na^+ are given in Table V together with the Li^7 and Na^{23} quadrupole moments and their magnetic resonance (NMR) frequencies, in a standard field of 10 kG. The quantities e^2qQ/h, which determine the first- and second-order quadrupole effects[27] on the NMR frequency are listed in Table VI. The $Z'Z'$ component of the field-gradient tensor corrected for antishielding effects will henceforth be denoted by q:

$$q=V_{z'z'}(1-\gamma_\infty). \tag{34}$$

For the $\langle 110\rangle$ case, the asymmetry parameter η is also required[27] for the evaluation of first- and second-order frequencies and is listed in Table VI.

The first-order frequency splitting of the NMR line $m\leftrightarrow m-1$ is given by

$$\nu_m{}^{(1)}=-A(1-\gamma_\infty)V_{zz}(m-\tfrac{1}{2}), \tag{35}$$

where

$$A=3e^2Q/2I(2I-1)h. \tag{36}$$

The second-order displacement in frequency of the same line is given by[4]

$$\begin{aligned}\nu_m{}^{(2)}=A^2(1-\gamma_\infty)^2\{&\tfrac{2}{3}(V_{zx}{}^2+V_{zy}{}^2)[24m(m-1)\\&-4I(I+1)+9]-\tfrac{1}{12}[(V_{xx}-V_{yy})^2+4V_{xy}{}^2]\\&\times[12m(m-1)-4I(I+1)+6]\}.\end{aligned} \tag{37}$$

In Eqs. (35) and (37) the field-gradient components are referred to a laboratory system with the z axis along the magnetic-field direction. These components can be obtained from the principal-axis components through the transformation relation Eq. (30). A knowledge of e^2qQ/h, η, and of the orientations of the principal-axis systems as listed in Tables III and VI is therefore sufficient to calculate $\nu_m{}^{(1)}$ and $\nu_m{}^{(2)}$. The nuclei considered here, Li^7 and Na^{23}, both have $I=\frac{3}{2}$ and thus one expects[27] to see first-order effects from the $\frac{3}{2}\leftrightarrow\frac{1}{2}$ and $-\frac{1}{2}\leftrightarrow-\frac{3}{2}$ transitions and second-order effects from the $\frac{1}{2}\leftrightarrow-\frac{1}{2}$ transitions. In analyzing the frequency splitting and shift effects of NMR lines in these systems, the quasirotational motion[10] must be taken into account. The frequency of the latter is about 1 cm^{-1} or 30 000 Mc/sec for KCl:Li^+, much greater than the quadrupolar frequencies anticipated from Table VI. One must therefore average the field-gradient tensor over all of the equivalent equilibrium positions encompassed by the quasirotational motion. Such an averaging will yield a vanishing field-gradient tensor in all three cases considered here. One therefore has to break the octahedral symmetry by restricting the tunneling motion if a quadrupole interaction is to be observed. Two possible ways of accomplishing this are by the application of an electric field or a uniaxial stress. In particular, if an electric field is applied along the [111] direction, the potential will be reduced to C_{3v} symmetry. Then rather than 8 equivalent $\langle 111\rangle$ minima, there will now be 4 distinct energies, the order [111], three $\langle 11\bar{1}\rangle$, three $\langle 1\bar{1}\bar{1}\rangle$, and $[\bar{1}\bar{1}\bar{1}]$ configurations. For a field on the order of 50 000 V/cm, using the calculated value of the dipole moment $\boldsymbol{\mu}$ for KCl:Li^+ in Table II, one finds an energy difference of about 0.002 eV separating adjacent energy levels. This is of the same order as the calculated difference of 0.008 eV between the field free $\langle 111\rangle$ and $\langle 110\rangle$ minima, which is a measure of the barrier height between equivalent $\langle 111\rangle$ minima. An electric field of 50 000 v/cm will therefore effectively restrict the tunneling motion. This may also be seen by comparing the interaction energy $\boldsymbol{\mu}\cdot\mathbf{E}$ in frequency units with the observed tunneling frequency[9] of 1 cm^{-1}. It is important to notice that this applied field causes negligible additional lattice distortion and therefore does not significantly alter the unaveraged field gradients in Table IV.

It will now be shown that the occurrence of first-order splittings of NMR lines for different relative orientations of applied electric and magnetic fields can distin-

TABLE V. Pertinent constants for nuclear quadrupole interaction.

Nucleus[a]	Quadrupole moment, Q (10^{-24} cm^2)	Antishielding factor for ion[b] $(1-\gamma_\infty)$	NMR frequency[c] $H=10\,000$ G (Mc/sec)
Li^7	−0.05	0.744	16.547
Na^{23}	+0.1	5.53	11.262

[a] Li^7—K. C. Brog, T. G. Eck, and H. Wieder, Phys. Rev. **153**, 91 (1967). Na^{23}—M. Perl, I. I. Rabi, and B. Senitzky, Phys. Rev. **98**, 611 (1955).
[b] T. P. Das and R. Bersohn, Phys. Rev. **102**, 733 (1956). See also R. M. Sternheimer and H. M. Foley, *ibid.* **102**, 731 (1956).
[c] NMR Tables, 4th ed., compiled by Varian Associates, Palo Alto, California (unpublished).

TABLE VI. Quadrupole coupling constants and asymmetry parameters.

	e^2qQ/h (Mc/sec)		η
		KCl:Li^7	
[111]	−0.1196		0
[110]	+0.0850		0.6374
[100]	+0.0283		0
		KBr:Li^7	
[111]	−0.0834		0
[110]	+0.0568		0.6950
[100]	+0.0393		0
		CsF:Na^{23}	
[111]	3.965		0
[110]	−1.789		0.6577
[100]	−1.584		0

[28] R. M. Sternheimer, Phys. Rev. **84**, 244 (1951).

TABLE VII. Dependence of field-gradient tensors on E-field directions.

Ion displacement direction \ Electric field direction	[111]	[110]	[100]
[111]	q finite along [111]. $\eta=0$	$q\neq0$ $\eta=0$	$q=0$ $\eta=0$
[110]	q finite along [111]. $\eta=0$	$q\neq0$ $\eta\neq0$	q finite along [100]. $\eta=0$
[100]	$q=0$ $\eta=0$	$q\neq0$ $\eta\neq0$	q finite along [100]. $\eta=0$

guish between the three configurations namely ζ_a along ⟨111⟩, ⟨110⟩, or ⟨100⟩.

Thus, besides providing additional data to check with theory, NMR measurements can lead to independent confirmation of the ζ_a orientation deduced from ultrasonic measurements. In this connection, it is necessary to derive the principal axis for different electric field directions. Let us consider as an example an electric field applied in the [111] direction. If ζ_a is along ⟨111⟩ then as discussed in the previous paragraph the Li^+ ion will be trapped along [111], leading to an axially symmetric field gradient in this direction. If ζ_a were along ⟨100⟩ the electric field would make the [100], [010], and [001] directions energetically favored. The Li^+ ion would thus experience the average of three axially symmetric field gradients along these three directions. Using the relation Eq. (30) to calculate this average it can be seen that the field gradient vanishes. For ζ_a along ⟨110⟩ the directions [110], [011], and [101], would be energetically favored, and using Eq. (30) the net field gradient may be shown to be axially symmetric along [111]. By arguments of this nature one obtains the characteristics of the field-gradient tensors listed in Table VII for the electric field along the three directions. Having determined the averaged field gradient tensor in the presence of the electric field, Eq. (30) can be used to transform to a laboratory system with z axis parallel to the applied magnetic field for the evaluation of first-order splittings $\nu_m^{(1)}$ in Eq. (32). For example, if the magnetic field is applied along the [100] direction while the electric field is in [111], and with ζ_a along ⟨111⟩, then from Table III the requisite direction cosine is $\cos\theta=1/\sqrt{3}$ and $V_{zz}\propto(3\cos^2\theta-1)=0$. Thus no first-order splitting is expected in this situation. On the other hand, with the electric field and ζ_a both along [111] one has $\theta=0$ and $V_{zz}\propto(3\cos^2\theta-1)=2$, leading to a finite first-order splitting. By such reasoning one can predict the occurrence or non-occurrence of first-order splittings in Table VIII for the 27 possible combinations of electric field, magnetic field, and ζ_a directions when these are restricted to [111], [110], and [100]. It is clear that by testing for the presence or absence of first-order NMR splitting for the combinations of electric and magnetic field directions in Table VIII, one can determine whether ζ_a is along ⟨111⟩, ⟨110⟩, or ⟨100⟩. A similar analysis can be applied to the second-order splitting of the $\frac{1}{2}\leftrightarrow-\frac{1}{2}$ line using Eq. (37) and Tables III and VII. Detection of these quadrupole splittings depends on two factors: the magnitude of the splitting frequency, and the intensity of the resonance signal. If the electric and magnetic fields, as well as the impurity displacement, are all along [111], then the values of $\nu_{3/2}^{(1)}$ are half the values of e^2qQ/h listed in Table VI for the ⟨111⟩ case. These are all sizable frequencies which are larger than the magnetic dipolar breadth. The NMR frequencies of both Na^{23} and Li^7 are sizable and so are their abundances, therefore resonances of Na^{23} and Li^7 in bulk systems are quite easy to detect. However, in CsF:Na^{23} and KCl:Li^7, dilute solid solutions have to be used if the theory of isolated impurities is to apply and this will weaken the intensity of the expected NMR lines for the impurity nucleus. The technique developed by Slusher and Hahn[2] of detecting less abundant nuclei through their interaction with an abundant nuclear spin species could be a suitable means of observing the impurity resonance when it is too weak to detect directly.

TABLE VIII. Description of first-order splitting for various E and H directions.[a]

E direction	H direction	Ion-displacement direction [111]	[110]	[100]
[111]	[111]	Yes	Yes	No
[111]	[110]	Yes	No	Yes
[111]	[100]	No	No	No
[110]	[111]	Yes	Yes	Yes
[110]	[110]	Yes	Yes	Yes
[110]	[101]	Yes	Yes	Yes
[100]	[111]	No	Yes	Yes
[100]	[110]	No	Yes	Yes
[100]	[100]	No	No	No

[a] A Yes entry represents first-order splitting of NMR line is expected to be observed, while No indicates that there should be no first-order splitting.

V. CONCLUSIONS

The results of our calculations show that off-center displacement of Li^+ in KCl follows naturally from the simple nearest-neighbor Born-Mayer treatment employed. The model yields the ⟨111⟩ minimum as the lowest in energy of the three directions tried: ⟨111⟩, ⟨110⟩, and ⟨100⟩. This is true for all three materials treated: KCl:Li^+, KBr:Li^+, and CsF:Na^+. The ⟨100⟩ energy was the highest in all three materials, but was still lower than the energy of the centrosymmetric configuration. Our results are in qualitative agreement with experiment, and the dipole moments and vibrational frequencies agree within about a factor of two with experiment. Considering the simplicity of this model,

it appears reasonable to conclude from its successes that the nearest-neighbor effects are the most important in promoting off-center displacement and in favoring the [111] direction. Quantitative agreement with experiment was not anticipated because of the approximate treatment of polarization and uncertainties in the choice of repulsive potential. It is believed that more accurate results can be expected if electronic calculations are carried out to include covalent and overlap effects between the electrons of the impurity and its nearest neighbors. To make such calculations as quantitative as possible, a Born-Mayer treatment for the other neighbors could also be incorporated into the improved model. Once reliable potential energy curves are determined through such mixed calculations, a quantitative analysis of motional effects could be attempted.

Our study of the strength of nuclear quadrupole interactions of the impurity nucleus with the field gradients produced by the surrounding neighbors indicates the feasibility of observing nuclear quadrupole effects on NMR frequencies. It is proposed that measurements of NMR spectra by conventional or special double-resonance techniques, using an electric field to inhibit rotational motion, would serve as an additional confirmation of the actual displacement direction already indicated by ultrasonic measurements.

Similar off-center minima are expected for small divalent impurity ions in alkaline-earth oxides. Possible examples are Mg^{++}, Mn^{++}, and Fe^{+++} in BaO. The Mn^{++} and Fe^{+++} ions are expected to be particularly interesting since an axial field term $D[3S_z^2-S(S+1)]$ would occur in the spin Hamiltonian for spin resonance and a nuclear quadrupole interaction could be detected in the Mössbauer spectra of Fe^{57}. Pure Born-Mayer-type calculations will probably be inadequate to determine the lattice configurations even qualitatively in these systems, owing to the great diffuseness of the O^{--} ions.

ACKNOWLEDGMENTS

The authors are grateful to Dr. S. K. Joshi, Dr. J. D. Lyons, and B. K. Rao for helpful discussions.

APPENDIX

In order to derive Eq. (7), the expression for the electrostatic energy ΔE_e, first consider that all ions are fixed at their respective lattice sites, giving $\Delta E_e=0$. Now consider that just one ion, say the impurity ion, is displaced from its site and has coordinates relative to this site of (ξ,θ,φ). The change in electrostatic energy is then found from the potential of this ion in the field produced by the surrounding perfect lattice, minus the Madelung potential this ion had when on its site. We call this potential $V_L(\xi_1,\theta_1,\varphi_1)$ and briefly describe in the main text a method for its evaluation. Now suppose that a second ion is displaced from its lattice site. Place a virtual charge pair $(\pm q_2)$ at its lattice site. The one which has the normal sign will restore the perfect lattice potential back at the first site, thus preserving the V_L $(\xi_1,\theta_1,\varphi_1)$ term. But now we must also include the interaction energy $-q_1q_2/r_{1'2}$ between the first displaced ion (at $\mathbf{r}_{1'}$) of charge q_1 and the virtual charge $-q_2$ at the second lattice site ($\mathbf{r}_2$). Similarly to find the interaction of ion 2 with the lattice, we place a virtual charge pair $(\pm q_1)$ at site $\mathbf{r}_1$ and thus restore the lattice to obtain a term V_L $(\xi_2,\theta_2,\varphi_2)$ along with an interaction $-q_1q_2/r_{12'}$ between the displaced ion 2 and the virtual charge $-q_1$ at $\mathbf{r}_1$. The two displaced ions also interact giving a term $q_1q_2/r_{1'2'}$. Finally the virtual charges of "abnormal" sign interact with each other to give a term q_1q_2/r_{12}. The result is that for each pair of charges which are displaced we will obtain the expression

$$\Delta E_e^{(12)}=q_1q_2\left(\frac{1}{r_{1'2'}}+\frac{1}{r_{12}}-\frac{1}{r_{12'}}-\frac{1}{r_{1'2}}\right)+q_1V_L(\xi_1,\theta_1,\phi_1)+q_2V_L(\xi_2,\theta_2,\phi_2). \quad \text{(A1)}$$

Then when all of the D ions have been displaced, we sum over all such pairs to obtain

$$\Delta E_e=\sum_{\substack{J\in D\\ J\neq K}}\sum_{K\in D} q_Jq_K\left(\frac{1}{r_{J'K'}}+\frac{1}{r_{JK}}-\frac{1}{r_{J'K}}-\frac{1}{r_{JK'}}\right)+\sum_{J\in D} q_JV_L(\xi_J,\theta_J,\phi_J) \quad \text{(A2)}$$

which is another form of Eq. (7), namely, Eq. (13).

It should be noted that this treatment was adopted by Das, Jette, and Knox[29] in an earlier work on color centers. Since they were only interested in up to quadratic terms in the displacement, they did not include the last term of Eq. (A2) in their calculations.

[29] T. P. Das, A. N. Jette, and R. S. Knox, Phys. Rev. 134, A1079 (1964).